

# Momentum Approximation in Asynchronous Private Federated Learning

Tao Yu<sup>1</sup> Congzheng Song<sup>2</sup> Jianyu Wang<sup>2</sup> Mona Chitnis<sup>2</sup>

## Abstract

Asynchronous protocols have been shown to improve the scalability of federated learning (FL) with a massive number of clients. Meanwhile, momentum-based methods can achieve the best model quality in synchronous FL. However, naively applying momentum in asynchronous FL algorithms leads to slower convergence and degraded model performance. It is still unclear how to effectively combine these two techniques together to achieve a win-win. In this paper, we find that asynchrony introduces implicit bias to momentum updates. In order to address this problem, we propose momentum approximation that minimizes the bias by finding an optimal weighted average of all historical model updates. Momentum approximation is compatible with secure aggregation as well as differential privacy, and can be easily integrated in production FL systems with a minor communication and storage cost. We empirically demonstrate that on benchmark FL datasets, momentum approximation can achieve 1.15–4× speed up in convergence compared to existing asynchronous FL optimizers with momentum.

## 1. Introduction

Practical deployment of synchronous federated learning (SyncFL) (McMahan et al., 2017) encounters scalability issue due to the requirement on global synchronization of clients’ model updates, wherein the central aggregation are contingent upon the completion of local training and communication across all participating clients. In order to address this issue, asynchronous FL (AsyncFL) (Xie et al., 2019; van Dijk et al., 2020; Park et al., 2021; Chai et al., 2021; Nguyen et al., 2022; Zhang et al., 2023) was proposed, which allows concurrent model updates at both the server and the clients’ side. One concrete example is FedBuff (Nguyen et al., 2022), which is the state-of-the-art AsyncFL method and has been deployed in many production systems (Huba et al., 2022; Wang et al., 2023). In each FedBuff iteration, the server first broadcasts the global model and triggers local training on  $K$  randomly sampled

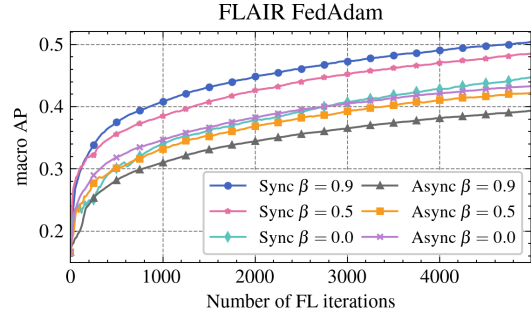


Figure 1. Negative impact of momentum in AsyncFL on the FLAIR dataset. In SyncFL, FedAdam with momentum parameter  $\beta = 0.9$  converges fastest while it is the opposite case in AsyncFL: no momentum ( $\beta = 0$ ) is better.

clients, then, receives clients’ local model updates in a buffer. Once the buffer reaches a target cohort size  $C \ll K$ , the server will directly proceed to the next iteration without waiting for the all  $K$  clients finish computation. As a result, the buffer gets filled up much quicker than SyncFL and the latency per iteration improves significantly (Dutta et al., 2021). However, since clients sampled in all previous iterations can contribute to the current global model update, AsyncFL methods typically have slower model convergence w.r.t iterations than SyncFL.

On the other hand, momentum-based optimizers such as momentum SGD and Adam have become dominant in the deep learning community due to their superior performance. Similar observations also appeared in SyncFL. For example, researchers found that applying momentum methods for the server model updates (e.g., FedAvgM (Hsu et al., 2019) and FedAdam (Reddi et al., 2020)) can greatly improve the final model quality and convergence speed.

Given the appealing benefits of asynchrony and momentum, it is desired to combine them to achieve a win-win in both efficiency and model quality. Unfortunately, the naive combination does not work. For instance, Mitliagkas et al. (2016); Zhang & Mitliagkas (2017) showed that sophisticated tuning of the momentum parameter  $\beta$  is very critical in asynchronous SGD (AsyncSGD). Rather than consistently using a larger  $\beta$  (e.g. 0.9) in the synchronous setting, a smaller or even negative  $\beta$  is preferred and the best value may vary across datasets. We observe the same phenomenon for AsyncFL. As shown in Figure 1, FedAdam

<sup>1</sup>Cornell University <sup>2</sup>Apple.

with  $\beta = 0.5$  and  $0.9$  underperforms  $\beta = 0$  case in asynchronous setting while the pattern is the opposite if updates are synchronous.

Many prior AsyncFL works proposed to down-scale the stale client updates before central aggregation to control the impact of staleness (Xie et al., 2019; Park et al., 2021). However, this does not help in combining asynchrony and momentum. As shown in the experiments of FedBuff (Nguyen et al., 2022), even with lower weights for stale updates, the momentum parameter still needs to be carefully tuned on different datasets and the best value can be 0 (i.e. no momentum). It remains an open question: *is it possible to effectively integrate asynchrony and momentum in FL to simultaneously harness the advantages in scalability and better model quality?*

**Contributions.** In this paper, we provide an affirmative answer to the above question. Motivated by the fact that momentum method itself utilizes all past gradients by taking an exponential average (i.e., has unbounded staleness), we argue that the key issue in applying momentum to AsyncFL may not be the large staleness of model updates. Instead, the real problem is that naive asynchronous momentum method does not properly exploit the past information. We demonstrate that asynchrony introduces implicit weight bias to past gradients and hence, removes the momentum effect.

In order to address this problem, we propose a new algorithm named *momentum approximation*, which solves a least square problem in each FL iteration  $t$  to find the best coefficients to weight the historical model updates before  $t$ , such that the weighted historical updates are close to the momentum updates as in the synchronous setting and thus retain the acceleration from momentum. We highlight some key features of this algorithm:

- Momentum approximation is compatible with any momentum-based federated optimizer and its convergence pattern behaves similar to SyncFL. It resolves the need of extensively tuning  $\beta$  from a wider range for different tasks in prior works. One can consistently set  $\beta$  found in SyncFL to get the best model quality in the AsyncFL.
- Momentum approximation can be easily integrated in production FL systems, and inherits all the benefits from FedBuff, such as its scalability, robustness and compatibility to privacy. It incurs only a minor communication of a iteration number in addition to model updates, and storage cost of historical updates on the server side.
- We empirically demonstrate that on two large-scale FL benchmarks, StackOverflow (Authors, 2019) and FLAIR (Song et al., 2022), momentum approximation achieves 1.15–4 $\times$  speed up in convergence and 3–20% improvements in utility compared to vanilla FedBuff with momentum.

## 2. Background

In federated learning (FL), we aim to train a model  $\theta \in \mathbb{R}^d$  with  $m$  clients collaboratively. In iteration  $t$  of FL, a cohort of clients is sampled and the server broadcasts the current global model  $\theta_t$  to the sampled clients  $\mathcal{K}_t$ . Each sampled client  $k$  trains on their local dataset, and then submits the model updates  $\Delta_k(\theta_t)$  before and after the local training back to the server. In SyncFL, the server waits for the local model updates from all  $K = |\mathcal{K}_t|$  clients and uses the *aggregated model updates* (defined as follows)

$$d_t = \frac{1}{K} \sum_{k \in \mathcal{K}_t} \Delta_k(\theta_t)$$

to update the global model before proceeding to the next iteration. More formally, synchronous federated averaging (FedAvg) (McMahan et al., 2017) algorithm updates the global model as follows:

$$\theta_{t+1} = \theta_t - \eta d_t,$$

where  $\eta$  denotes the server learning rate.

**Momentum-based optimizers.** In practice, momentum-based optimizers (Wang et al., 2019a; Hsu et al., 2019; Reddi et al., 2020) on the server side are often more preferred than FedAvg as they can either greatly accelerate convergence or improve the final model quality given a fixed iteration budget. We denote these optimizers as SERVEROPT, and the update rule of which can be formulated as:

$$m_t = \beta m_{t-1} + (1 - \beta) d_t, \theta_{t+1} = \theta_t - \eta H_t^{-1} m_t, \quad (1)$$

where  $\beta \in [0, 1)$  is the momentum parameter and  $m_t$  is the momentum buffer.  $H_t^{-1}$  is the preconditioner where  $H_t = I_d$  in FedAvgM (Hsu et al., 2019), and  $H_t$  is the square root of accumulated or exponential moving average of  $d_t$ 's second moments in adaptive optimizers such as FedAdaGrad and FedAdam (Duchi et al., 2011; Kingma & Ba, 2015; Reddi et al., 2020).

**FL with differential privacy.** Though the clients' raw data is never shared with the server in FL, the model updates  $d_t$  can still reveal sensitive information about the clients (Melis et al., 2019; Zhu et al., 2019; Nasr et al., 2019). Differential privacy (DP) is a standard approach to prevent leakage from model updates and provide a meaningful privacy guarantee.

**Definition 2.1** (Differential Privacy (Dwork et al., 2006b)). A randomized algorithm  $\mathcal{A} : \mathcal{D} \mapsto \mathcal{R}$  is  $(\epsilon, \delta)$ -differentially private, if for any pair of neighboring training populations  $\mathcal{D}$  and  $\mathcal{D}'$  and for any subset of outputs  $\mathcal{S} \subseteq \mathcal{R}$ , it holds that

$$\Pr[\mathcal{A}(\mathcal{D}) \in \mathcal{S}] \leq e^\epsilon \cdot \Pr[\mathcal{A}(\mathcal{D}') \in \mathcal{S}] + \delta. \quad (2)$$

We consider client-level DP where a training population  $\mathcal{D}'$  is the neighbor of  $\mathcal{D}$  if  $\mathcal{D}'$  can be obtained by adding or removing one client from  $\mathcal{D}$ , and vice versa.

Gaussian Mechanism (Dwork et al., 2006a) can be easily combined with FL (McMahan et al., 2018) to enable DP, where two more additional steps are required in each iteration: (1) each client model update is clipped by  $\text{clip}(\Delta_k, S) = \Delta_k \cdot \min(1, S/\|\Delta_k\|_2)$  with  $L^2$  sensitivity bound  $S$ , and (2) the aggregated clipped model updates are added with Gaussian noise as  $\sum_k \text{clip}(\Delta_k, S) + \mathcal{N}(0, \sigma^2 S^2 \mathbf{I}_d)$  where  $\sigma$  is calibrated from a standard privacy accountant such as Rényi DP (Mironov, 2017). We also assume a secure aggregation protocol is used so that the server learns only the sum  $\sum_k \Delta_k$  but never the individual model updates  $\Delta_k$  (Bonawitz et al., 2017; Huba et al., 2022; Talwar et al., 2023).

**Client subsampling and privacy amplification.** When the number of clients is massive, subsampling of clients improves the training efficiency in each iteration. There are many different ways to implement client subsampling. In this work, we focus on client-side Poisson sampling:

**Definition 2.2** (Poisson sampling (Zhu & Wang, 2019)). Given  $m$  clients, Poisson sampling outputs a subset of the clients  $\mathcal{K} = \{k | Z_k = 1, k \in [m]\}$  by sampling  $Z_k \sim \text{Bernoulli}(q)$  independently for  $k = 1, \dots, m$ .

Poisson sampling is easy to implement in production FL systems (Paulik et al., 2021), where each client flips a biased coin with probability  $q$  and decides to participate training if the coin comes up head.

Another benefit of Poisson sampling is that it enjoys privacy amplification by subsampling (Abadi et al., 2016; McMahan et al., 2018; Zhu & Wang, 2019; Mironov et al., 2019), i.e. the privacy guarantee is amplified to  $(\mathcal{O}(q\epsilon), q\delta)$ . Other sampling methods, such as sampling without replacement on the server (Bonawitz et al., 2019), are hard to achieve uniformly at random in practice as the population of available clients is dynamic, and thus the guarantee from amplification by subsampling might not hold (Kairouz et al., 2021).

### 3. Applying Momentum to Asynchronous FL

In this section, we first demonstrate the problem in naively combining momentum and AsyncFL, and then introduce momentum approximation to address it. The key idea is to carefully adjust the weight of each past (pseudo-) gradients to make them approximate the desired momentum updates. Unless otherwise stated, we focus on the FedBuff algorithm, which is a general and state-of-the-art AsyncFL algorithm.

**Notation.** For a matrix  $\mathbf{A}$ , we use  $\mathbf{A}_{[i,:]}$  to denote  $i$ -th row,  $\mathbf{A}_{[:,j]}$  the  $j$ -th column, and  $\mathbf{A}_{[i,j]}$  the  $(i, j)$ -th entry of  $\mathbf{A}$ . We denote the staleness as  $\tau(k)$  for client  $k$ , i.e.  $k$  is sampled at iteration  $t - \tau(k)$  and their updates is received at  $t$ . We let  $\mathbf{e}_i \in \{0, 1\}^T$  denote the binary one-hot encoding vector where all entries are 0 except for the  $i$ -th entry being 1, and  $\mathbf{1} = [1, 1, \dots, 1]^T$  denote a vectore with all ones.

#### 3.1. Implicit Momentum Bias

In order to get a better understanding on the convergence issue of AsyncFL with momentum, we first present a general update rule for FL and then compare synchronous momentum methods and asynchronous ones as special cases.

Without loss of generality, we define  $\mathbf{r}_t \in \mathbb{R}^d$  as the aggregated pseudo-gradient (or model updates) received by the server at iteration  $t$ , and denote  $\mathbf{R} = [\mathbf{r}_1, \mathbf{r}_2, \dots, \mathbf{r}_T] \in \mathbb{R}^{d \times T}$ . Then, the following proposition holds (Denisov et al., 2022).

**Proposition 3.1.** *Suppose the server model  $\theta$  is updated using momentum method as follows:*

$$\mathbf{m}_t = \beta \mathbf{m}_{t-1} + (1 - \beta) \mathbf{r}_t, \quad \theta_{t+1} = \theta_t - \eta \mathbf{m}_t.$$

*This update rule is equivalent to  $\theta_{t+1} = \theta_t - \eta(1 - \beta) \sum_{s=1}^t \beta^{t-s} \mathbf{r}_s$ . The final model after total  $T$  iterations can be written as*

$$\theta_{T+1} = \theta_1 - \eta \mathbf{R} \mathbf{M}^T \mathbf{1} \quad (3)$$

where  $\mathbf{M} \in \mathbb{R}^{T \times T}$  is a lower-triangular matrix defined as:

$$\mathbf{M}_{[t,s]} = \begin{cases} \beta^{t-s}(1 - \beta) & \text{if } t \geq s \\ 0 & \text{otherwise} \end{cases}. \quad (4)$$

With the above general update rule, both SyncFL and AsyncFL can be treated as special cases. For SyncFL, the received (pseudo-) gradient on server is just the aggregated local model updates from clients, that is,  $\mathbf{r}_t = \mathbf{d}_t$  and

$$\theta_{T+1}^{\text{sync}} = \theta_1 - \eta \mathbf{D} \mathbf{M}^T \mathbf{1}, \quad (5)$$

where  $\mathbf{D} = [\mathbf{d}_1, \mathbf{d}_2, \dots, \mathbf{d}_T]$ .

For asynchronous setting, the concrete expression of  $\mathbf{r}_t$  is more complicated. At each iteration of FedBuff, the server broadcasts the latest model  $\theta_t$  to  $K$  random sampled clients to trigger local training and applies a global update after receiving  $C$  local model updates from a set of clients  $\mathcal{C}_t$ . However, these received local model updates can be stale. Let  $C_{t,s} \geq 0$  denote the number of received clients' updates at iteration  $t$  from iteration  $s$  and  $\sum_{s=1}^t C_{t,s} = C$ . Then, the current (pseudo-) gradient on server can be written as a weighted average of all past updates:

$$\mathbf{r}_t = \sum_{s=1}^t \frac{C_{t,s}}{C} (\mathbf{d}_s + \zeta_{t,s}) \quad (6)$$

where  $\mathbf{d}_s$  has the same definition as of in the synchronous setting: the aggregated local model updates initialized from stale model  $\theta_s$  from all  $K$  sampled clients. Besides, since the server only receives a subset of  $C_{t,s}$  individual local updates out of the sampled  $K$  clients at iteration  $s$ , there is an extra sampling error. We denote it as  $\zeta_{t,s}$ .

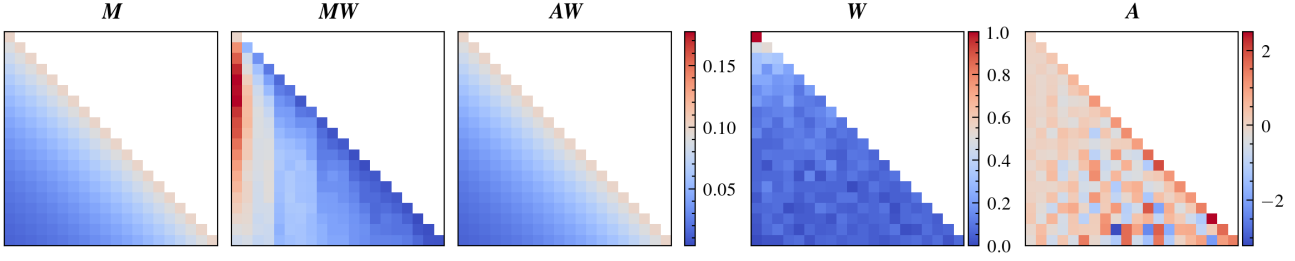


Figure 2. Visualization of the desired momentum matrix  $M$  ( $\beta = 0.9$ ), the implicit momentum matrix  $MW$ , the approximated momentum matrix  $AW$ , the staleness coefficient matrix  $W$ , and the solved weighting matrix  $A$  in momentum approximation.

We can define a weight matrix similar to  $M$ :

$$W_{[t,s]} = \begin{cases} C_{t,s}/C & \text{if } t \geq s \\ 0 & \text{otherwise.} \end{cases}$$

Then, one can easily derive that

$$R = DW^\top + E \quad (7)$$

where the  $t$ -th column of error matrix  $E$  is defined as  $\sum_{s=1}^t \frac{C_{t,s}}{C} \zeta_{t,s}$ . Substituting (7) back into (3), we get

$$\begin{aligned} \theta_{T+1}^{\text{async}} &= \theta_1 - \eta DW^\top M^\top \mathbf{1} - \eta EM^\top \mathbf{1} \\ &= \theta_1 - \eta D \left[ M^\top + \underbrace{(MW - M)^\top}_{\text{implicit momentum bias}} \right] \mathbf{1} \\ &\quad - \underbrace{\eta EM^\top \mathbf{1}}_{\text{async. sampling noise}}. \end{aligned} \quad (8)$$

Comparing the update rules Equations (5) and (8), there are two additional terms in asynchronous setting. One is the implicit momentum bias: the algorithm implicitly assigns biased weights  $MW$  (which is different from normal momentum weight  $M$ ) to historical gradients, losing the benefits of momentum acceleration. We provide a visualization of  $M$  and  $MW$  in Figure 2. While the normal momentum assigns the largest weight to the most recent gradients, asynchronous momentum tends to weigh more towards stale gradients, as they arrive more frequently.

Previous works (Mitliagkas et al., 2016) also observed that giving additional lower weights (e.g. exponential w.r.t. staleness) to historical gradients can help convergence. This phenomenon can be intuitively explained by the definition of implicit momentum bias, which becomes smaller when  $W$  approaches to the identity matrix. However, this approach cannot entirely solve the problem. It is nearly impossible to set  $W = I$  in realistic settings, as the gradients in current iteration may only arrive in future iterations.

The second additional term in Equation (8) is the asynchronous sampling noise: the server requested  $K$  clients

---

### Algorithm 1 FedBuff with Momentum Approximation

---

**Inputs:** client Poisson sampling rate  $q$ , cohort size  $C$ , server optimizer SERVEROPT, server learning rate  $\eta$ , number of FL iterations  $T$ , client local learning rate  $\eta_l$ , number, number of client local SGD steps  $Q$

**for**  $t = 1, \dots, T$  **do**

$\mathcal{K}_t \leftarrow$  sampled clients with Poisson sampling rate  $q$

Run CLIENT( $\theta_t, t$ ) for  $k \in \mathcal{K}_t$  asynchronously

**if** receives  $\Delta_k(\theta_{t-\tau(k)})$  and  $e_{t-\tau(k)}$  from  $k$  **then**

$r_t \leftarrow r_t + \frac{1}{C} \Delta_k(\theta_{t-\tau(k)})$

$W_{[t,:]} \leftarrow W_{[t,:]} + \frac{1}{C} e_{t-\tau(k)}^\top$

**if** server received  $C$  local model updates **then**

**if** light-weight momentum approximation **then**

$u_t, v_t \leftarrow$  solve Equation (15)

$\tilde{m}_t \leftarrow v_t \tilde{m}_{t-1} + u_t r_t$

**else**

$R_{[:,t]} \leftarrow r_t$  update the pseudo-gradient history

$a_t \leftarrow$  solve Equation (11)

$\tilde{m}_t \leftarrow R a_t$

$H_t \leftarrow$  update based on SERVEROPT

$\theta_{t+1} \leftarrow \theta_t - \eta H_t^{-1} \tilde{m}_t$

$r_{t+1}, W_{[t+1,:]} \leftarrow \mathbf{0}$

---

**function** CLIENT( $\theta, t$ )

$\theta' \leftarrow$  run  $Q$  SGD steps with  $\eta_l$  on local data

$e_t \leftarrow$  one-hot encoding of  $t$

Upload  $\Delta = \theta - \theta'$  and  $e_t$  to server

---

from  $s$ -th iteration but can only received  $C_{t,s}$  from the cohort at iteration  $t$ . We provide a basic analysis on the impact of this term in Appendix A.1. We leave a more thorough investigation of the sampling error for future studies and mainly focus on implicit momentum bias in this paper.

### 3.2. Proposed Method: Momentum Approximation

From Equation (6), note that, in asynchronous setting, the received (pseudo-) gradient  $r_t$  is already a weighted average of historical gradients. Therefore, instead of naively applying momentum on top of it, can we simply adjust the weights to imitate the momentum updates? Following this idea, we propose a new update rule for AsyncFL:

$$\theta_{t+1} = \theta_t - \eta R a_t, \quad (9)$$

where  $\mathbf{a}_t \in \mathbb{R}^T$  is an arbitrary vector weighting the aggregated model updates. Accordingly, we have

$$\begin{aligned}\boldsymbol{\theta}_{T+1}^{\text{MA}} &= \boldsymbol{\theta}_1 - \eta \mathbf{R} \mathbf{A}^\top \mathbf{1} = \boldsymbol{\theta}_1 - \eta \mathbf{D} \mathbf{W}^\top \mathbf{A}^\top \mathbf{1} - \eta \mathbf{E} \mathbf{A}^\top \mathbf{1} \\ &= \boldsymbol{\theta}_1 - \eta \mathbf{D} [\mathbf{M}^\top + (\mathbf{A} \mathbf{W} - \mathbf{M})^\top] \mathbf{1} - \eta \mathbf{E} \mathbf{A}^\top \mathbf{1},\end{aligned}\quad (10)$$

where  $\mathbf{A}^\top = [\mathbf{a}_1, \mathbf{a}_2, \dots, \mathbf{a}_T]$ . One can choose a matrix  $\mathbf{A}$  such that  $\mathbf{A} \mathbf{W} = \mathbf{M}$ . As a result, the implicit momentum bias is entirely removed. The resulting algorithm imitates or approximates the synchronous momentum method without explicitly adjusting momentum. For this reason, we name the proposed method as *momentum approximation (MA)*.

**Implementation.** The practical implementation of the proposed algorithm is very straightforward. Thanks to the lower-triangular nature of both matrices  $\mathbf{W}$  and  $\mathbf{M}$ , we can approximate the momentum matrix  $\mathbf{M}$  row-by-row, i.e., in an online fashion. At iteration  $t$ , the desired weights for past gradients are given as the  $t$ -th row of  $\mathbf{M}$  and known beforehand. We seek to optimize the following objective to find the best  $\mathbf{a}_t = \mathbf{a}_{\text{opt}}$  to be used in Equation (9):

$$\begin{aligned}\min_{\mathbf{a} \in \mathbb{R}^T} \|\mathbf{a}^\top \mathbf{W} - \mathbf{M}_{[t,:]} \|_2^2 \quad (11) \\ \text{subject to } \mathbf{a}_{[s]} = 0, \forall s > t.\end{aligned}$$

In each vector  $\mathbf{a}_t$ , only the first  $t$  elements are non-zero such that matrix  $\mathbf{A}$  is enforced to be an lower-triangular matrix. This is because the server cannot use gradients from future iterations. Solving Equation (11) requires knowing  $\mathbf{W}_{[t,:t]}$  (the first  $t$  rows and columns of  $\mathbf{W}$ ) which can be obtained by having each received client  $k$  to upload a one-hot encoding  $\mathbf{e}_s \in \{0, 1\}^T$  of their model version  $s$ . More concretely, suppose at iteration  $t$ , the received updates at server are from a subset of  $C$  clients and their model version are denoted as  $\{t - \tau(k)\}_{k \in C_t}$ . Then, the matrix  $\mathbf{W}$  is initialized with all 0 and updated online as  $\mathbf{W}_{[t,:]} = \frac{1}{C} \sum_{k \in C_t} \mathbf{e}_{t-\tau(k)}^\top$ . Sending the extra  $\mathbf{e}_{t-\tau(k)}$  adds a negligible communication cost as  $\mathbf{e}_{t-\tau(k)}$  has a payload size of  $T$  bits and  $T \ll d$  for common FL tasks.

**Light-weight momentum approximation.** The full approximation above requires a server-side storage cost of  $\mathcal{O}(Td)$  as all past received gradients  $\mathbf{R}$  needs to be saved. This is usually not a concern for FL since  $T$  is typically in the order of thousands and the model size  $d$  is small to meet on-device resource constraints (Xu et al., 2023b;a).

In the case of both  $T$  and  $d$  are high and the storage cost becomes a concern, we propose a light-weight approximation which has no extra storage cost on the server. The light-weight update rule is the same as Equation (9) except that  $\mathbf{a}_t$  is replaced by  $\tilde{\mathbf{a}}_t$  defined recursively as below:

$$\tilde{\mathbf{a}}_t = u_t \mathbf{e}_t + v_t \tilde{\mathbf{a}}_{t-1}, \quad (12)$$

where  $u_t, v_t \in \mathbb{R}$  are to be optimized. The recursive definition of  $\tilde{\mathbf{a}}_t$  allows us to rewrite Equation (9) as:

$$\begin{aligned}\boldsymbol{\theta}_{t+1} &= \boldsymbol{\theta}_t - \eta \mathbf{R} \tilde{\mathbf{a}}_t = \boldsymbol{\theta}_t - \eta (u_t \mathbf{R} \mathbf{e}_t + v_t \mathbf{R} \tilde{\mathbf{a}}_{t-1}) \\ &= \boldsymbol{\theta}_t - \eta (u_t \mathbf{r}_t + v_t \mathbf{R} \tilde{\mathbf{a}}_{t-1}),\end{aligned}\quad (13)$$

which can be simplified to the following update rule similar to Equation (1):

$$\tilde{\mathbf{m}}_t = \mathbf{R} \tilde{\mathbf{a}}_t = u_t \mathbf{r}_t + v_t \tilde{\mathbf{m}}_{t-1}, \quad \boldsymbol{\theta}_{t+1} = \boldsymbol{\theta}_t - \eta \tilde{\mathbf{m}}_t. \quad (14)$$

Since Equation (14) depends on  $\tilde{\mathbf{m}}$  and not on  $\mathbf{R}$ , light-weight approximation saves the extra  $\mathcal{O}(Td)$  storage cost and has the same space complexity as the standard momentum updates by maintaining a single buffer  $\tilde{\mathbf{m}}_t$ .

To find the best  $(u_t, v_t) = (u_{\text{opt}}, v_{\text{opt}})$  in iteration  $t$ , we can substitute (12) back into (11):

$$\min_{u, v \in \mathbb{R}} \|(u \mathbf{e}_t + v \tilde{\mathbf{a}}_{t-1})^\top \mathbf{W} - \mathbf{M}_{[t,:]} \|_2^2. \quad (15)$$

As we only optimize two scalars in each iteration, we expect the solution from light-weight approximation is sub-optimal compared to the full approximation in Equation (11).

**Differentially private momentum approximation.** Both the model updates  $\Delta_k$  and the model version one-hot encoding  $\mathbf{e}_{t-\tau(k)}$  are sensitive information as they reveal the client's local data and their timing of participating FL. We can use DP mechanisms to protect both information.

Let  $\gamma$  be a scaling factor and  $\mathbf{y}_k = \Delta_k \oplus \gamma \mathbf{e}_{t-\tau(k)} \in \mathbb{R}^{d+T}$  be the payload that client  $k$  intends to send to the server, where  $\oplus$  denotes vector concatenation. We constrain the  $L^2$  sensitivity of  $\mathbf{y}_k$  as:

$$\bar{\mathbf{y}}_k = \text{clip}(\Delta_k, S_\Delta) \oplus \gamma \mathbf{e}_{t-\tau(k)}, \quad (16)$$

such that  $\|\bar{\mathbf{y}}_k\|_2 \leq \sqrt{S_\Delta^2 + \gamma^2} = S$ . Applying Gaussian Mechanism as  $\sum_k \bar{\mathbf{y}}_k + \mathcal{N}(0, \sigma^2 S^2 \mathbf{I}_{d+T})$  satisfies  $(\epsilon, \delta)$ -DP as described in Section 2. By choosing  $\gamma = \frac{\sigma}{\sqrt{\xi^2 - \sigma^2}} S_\Delta$ , the Gaussian noise added to the un-scaled  $\sum_k \mathbf{e}_{t-\tau(k)}$  is  $\mathcal{N}(0, (\frac{\sigma}{\gamma} S)^2 \mathbf{I}_T)$  with standard deviation:

$$\frac{\sigma}{\gamma} S = \frac{\sigma}{\gamma} \sqrt{S_\Delta^2 + \gamma^2} = \sqrt{\frac{\sigma^2 (\xi^2 - \sigma^2)}{\sigma^2} + \sigma^2} = \xi. \quad (17)$$

In practice, we tune  $\xi > \sigma$  to balance the utility on  $\sum_k \Delta_k$  and  $\sum_k \mathbf{e}_{t-\tau(k)}$ . As momentum approximation is a post-processing (Dwork & Roth, 2014) on the private aggregates:

$$\mathbf{r}_t = \frac{1}{C} \left[ \sum_{k \in C_t} \text{clip}(\Delta_k, S_\Delta) + \mathcal{N}(0, \sigma^2 S^2 \mathbf{I}_d) \right], \quad (18)$$

$$\mathbf{W}_{[t,:]} = \frac{1}{C \gamma} \left[ \sum_{k \in C_t} \gamma \mathbf{e}_{t-\tau(k)}^\top + \mathcal{N}(0, \sigma^2 S^2 \mathbf{I}_T) \right], \quad (19)$$

the MA update rules in Equations (9) and (14) also satisfies the same  $(\epsilon, \delta)$ -DP guarantee.

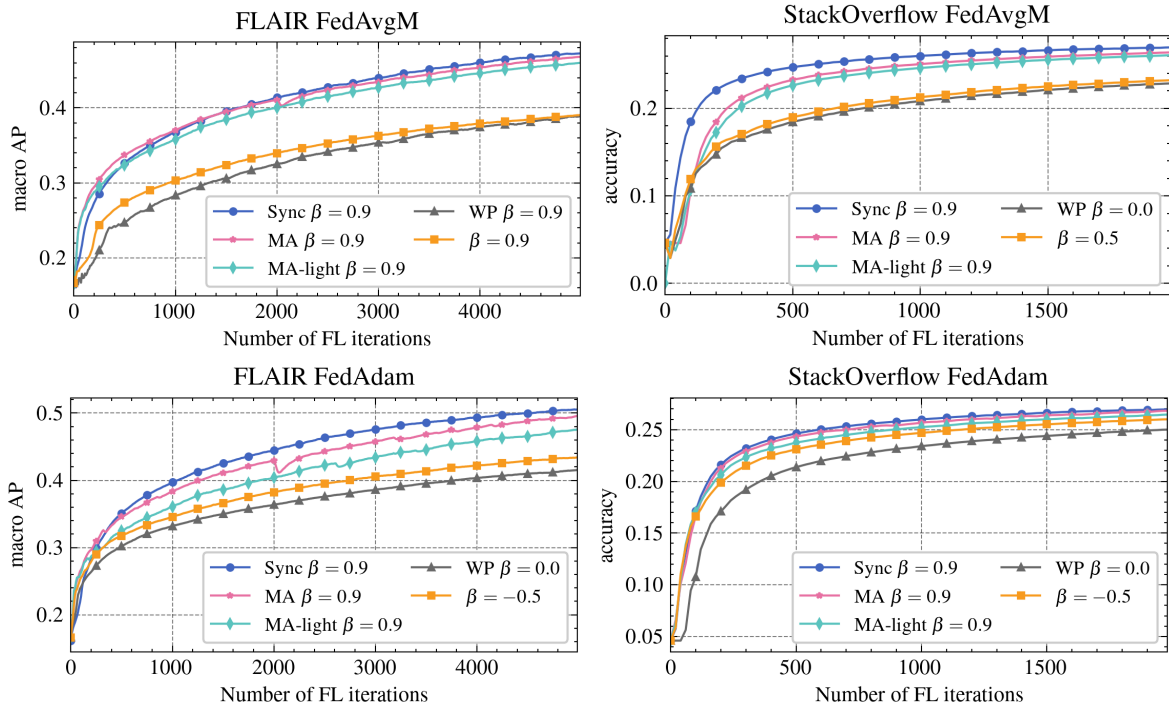


Figure 3. Comparison between momentum approximation (MA) and baseline approaches.

## 4. Experiments

In this section, we describe the experimental setup to evaluate momentum approximation (MA) with FedBuff and the results. We denote the light-weight MA in Equation (15) as MA-light. We focus on two SERVEROPT: FedAvgM (Hsu et al., 2019) and FedAdam (Reddi et al., 2020).

**Client delay distribution.** Following Nguyen et al. (2022), we adopt half-Normal distribution to model the client delay distribution. We demonstrate the impact of different client delay distributions on MA in Appendix B.3.

**Staleness scaling and bounding.** To mitigate the impact of staleness, we apply down-scaling on the client’s updates (Xie et al., 2019; Park et al., 2021; Nguyen et al., 2022) as  $1/(1 + \tau(k))^p \Delta_k$ , where  $p$  is a hyper-parameter (tuned between 0.5 to 2.0) controlling strength of the scaling. We further set a maximum staleness bound  $\tau_{\max}$  (default to 20) and drop  $\Delta_k$  if  $\tau(k) > \tau_{\max}$ .

**Datasets and ML Tasks.** We conduct experiments on FLAIR (Song et al., 2022), a large-scale annotated image dataset for multi-label classification, and StackOverflow (Authors, 2019), a commonly used language modeling FL benchmark dataset. Both datasets have real client partition and thus naturally capture the non-IID characteristics in real world FL setting.

For the FLAIR dataset, the task is to predict the set of coarse-

grained labeled objects in a given image. We use macro averaged precision (macro AP) as the evaluation metric. For the StackOverflow dataset, the task is next word prediction and we use top prediction accuracy as the evaluation metric following prior work (Reddi et al., 2020). The details of hyperparameter choices are described in Appendix B.1

### 4.1. Baselines

**Tuning for optimal momentum parameter.** As suggested in (Mitliagkas et al., 2016; Nguyen et al., 2022),  $\beta$  needs to be tuned carefully in AsyncFL and sometimes negative  $\beta$  performs better. We tune  $\beta$  from the range  $(-1, 1)$ .

**Weight prediction (WP).** WP is proposed to speed up AsyncSGD (Kosson et al., 2021) and in particular, to address the implicit momentum issue (Hakimi et al., 2019) in traditional distributed training setting. We modify WP to be compatible with AsyncFL as detailed in Appendix B.2.

### 4.2. Results

Figure 3 summarizes the convergence comparison between our proposed MA and the baseline approaches. For both FedAvgM and FedAdam on both datasets, MA and MA-light significantly outperforms the baseline approaches of best tuned  $\beta$ . We do not find WP worked well in the FL setting and acknowledge that more thoughtful integration is required to adopt techniques from AsyncSGD literature to

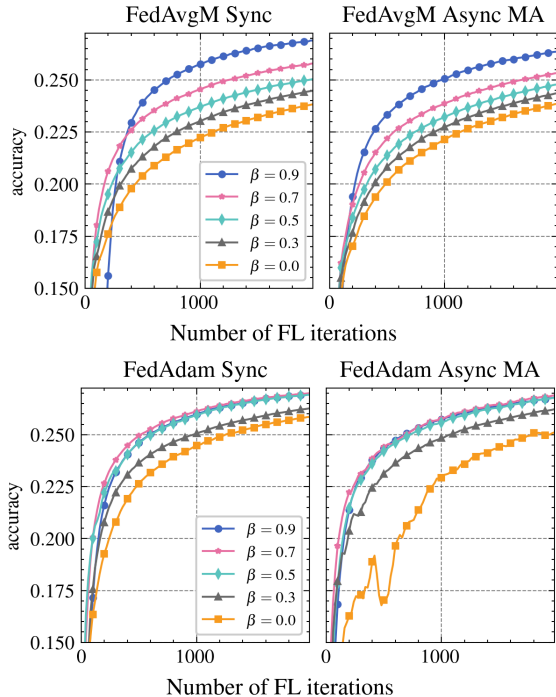


Figure 4. Impact of  $\beta$  on SyncFL and AsyncFL with MA on the StackOverflow dataset.

AsyncFL, which is beyond the scope of this work.

**Impact of  $\beta$ .** Figure 4 illustrates how  $\beta$  impacts SyncFL and AsyncFL with MA. The correlation pattern between  $\beta$  and the performance remains the same between SyncFL and AsyncFL with MA, i.e., larger  $\beta$  leads to better performance in this task. This demonstrates that the AsyncFL with MA can reuse the tuned  $\beta$  in SyncFL experiments instead of searching in a wider range from scratch, which saves the costs from expensive hyperparameter tuning in FL.

**Impact of cohort size.** Smaller cohort can negatively impact the convergence of MA as the variance of  $r_t$  in Equation (6) increases. We evaluate the impact of cohort size  $C$  on the StackOverflow dataset by varying  $C$  from 50 to 400. We compare the performance between SyncFL and FedBuff with MA on the same  $C$ . Table 1 shows the impact of  $C$  on MA. As  $C$  increases from 50 to 400, the gap between AsyncFL with MA and SyncFL becomes smaller, which validates our hypothesis that smaller cohort size has more negative impacts on MA than SyncFL.

**DP results.** Figure 5 illustrates the convergence results with DP. The pattern of the performance comparison is similar to that of the non-private case where both MA and MA-light outperform the AsyncFL baselines. We notice that in FedAdam baseline, negative  $\beta$  values are optimal on both datasets, indicating that the baseline approach requires more hyper-parameter tuning in a wider range of  $\beta$ .

$C$	FedAvgM		FedAam	
	MA	MA-light	MA	MA-light
50	5.17	7.68	7.26	11.94
100	3.17	4.25	2.47	4.51
200	2.18	3.44	0.52	1.87
400	1.39	2.8	0.46	0.4

Table 1. Relative accuracy gap (%) between SyncFL and AsyncFL with MA for different cohort sizes  $C$  on the StackOverflow dataset.

Setup	FedAvgM		FedAam	
	MA	MA-light	MA	MA-light
FLAIR	3.56×	3.01×	2.20×	1.66×
with DP	2.57×	2.09×	1.61×	1.15×
StackOverflow	3.96×	3.30×	1.62×	1.30×
with DP	2.06×	1.80×	1.50×	1.55×

Table 2. Relative speed up of MA compared to FedBuff baseline.

**Speed up of MA.** We finally evaluate the speed up of MA. Following (Nguyen et al., 2022), we record the iterations that MA needed to achieve the best metric from FedBuff baseline, and have this number divided by the iterations the baseline took to get the relative speed up. Table 2 summarizes the results. On both FLAIR and StackOverflow, MA speeds up FedAvgM more than FedAdam, and we suspect the reason is that the preconditioner in the FedAdam baseline is less affected, thereby mitigating the impact of staleness. Thus the improvement from MA is less significant. DP also impacts the speed up negatively as the estimation of  $\mathbf{W}$  becomes noisy and the noise scale on  $r_t$  increases.

## 5. Related Work

**Asynchronous distributed SGD.** The negative impact of gradient staleness has been studied in the traditional AsyncSGD setting. A line of research focused on reducing the impact of staleness or the discrepancy between worker’s model and the central model. Zhang et al. (2016) first proposed to down-scale the stale gradients based on their staleness  $\tau$ . Barkai et al. (2019) argued that  $\tau$  failed to accurately reflect the discrepancy and proposed to schedule down-scale based on the similarity between worker’s model and the central model. Zheng et al. (2017) used a Taylor expansion and Hessian approximation to compensate for the staleness. Hakimi et al. (2019); Kosson et al. (2021) proposed parameter prediction of the future central model to reduce discrepancy, simply by following the optimization oracle for more iterations. The impact of staleness is exacerbated by momentum, as analyzed in (Mitliagkas et al., 2016), where a small or even negative momentum parameter is preferred to adverse effects of asynchrony, which motivated an adaptive momentum training schedule (Zhang & Mitliagkas, 2017).

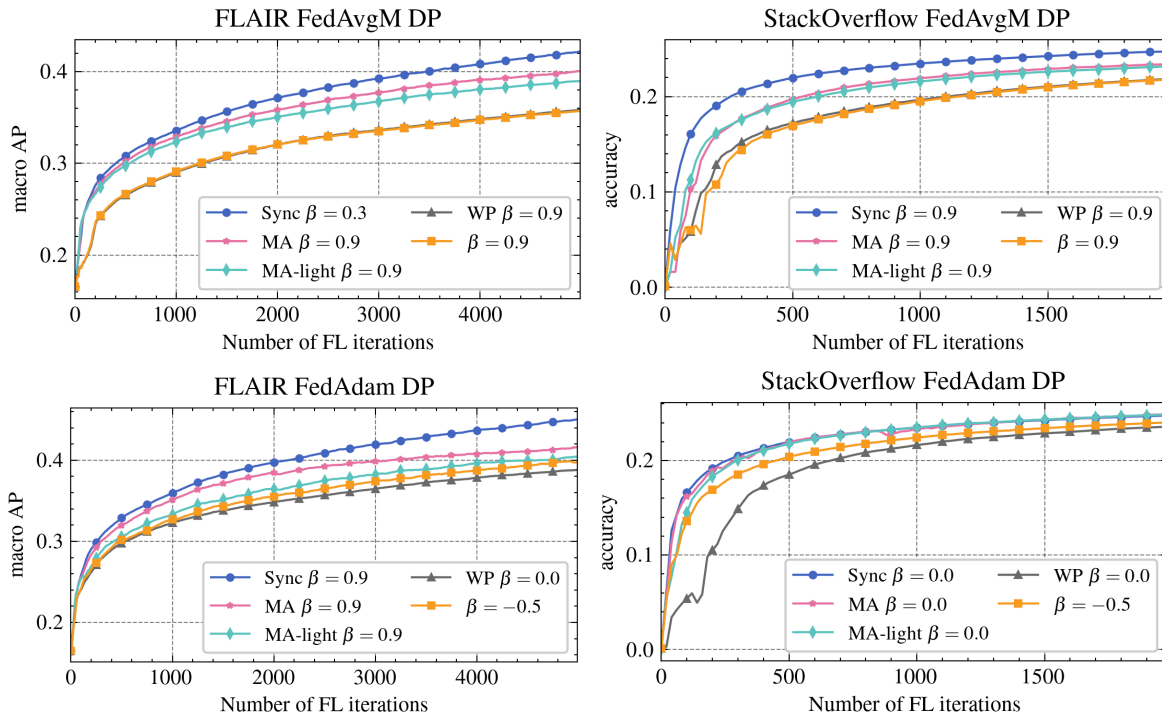


Figure 5. Comparison between momentum approximation (MA) and baseline approaches with differential privacy (DP).

**Asynchronous federated learning.** Existing AsyncFL works draw inspirations from AsyncSGD to handle stragglers and heterogeneous latency. Xie et al. (2019); Park et al. (2021); Nguyen et al. (2022) down-scaled the local model updates based on staleness  $\tau$  before the central aggregation. Nonetheless, as we showed, stale updates after down-scaling still affect training performance of momentum in practice.

On the other hand, FL differs from the traditional distributed SGD setting by having massive number of clients, higher communication overhead and more complicated system for secure aggregation and DP. Hence, many AsyncSGD algorithms do not directly fit in AsyncFL. Gradient compensation (Zheng et al., 2017) applied complicated operations on individual client updates, which is less obvious how to implement with secure aggregation. Hakimi et al. (2019); Chen et al. (2020); Kosson et al. (2021) required broadcasting model parameters and momentum, leading to doubled communication cost. Further research is needed to study how to integrate the other promising AsyncSGD algorithms efficiently in AsyncFL.

Apart from aforementioned AsyncFL algorithms on weight aggregation, there are many orthogonal tactics on improving AsyncFL. For example, gradient compression techniques (Li et al., 2020; Lu et al., 2020) improved communication efficiency; and model splitting (Chen et al., 2019; Wang et al., 2021b; Dun et al., 2023) had each client responsible for training a certain part of the whole model.

**Momentum-based federated optimizers.** Hsu et al. (2019) first proposed to extend FedAvg with server-side momentum (FedAvgM) to accelerate convergence. Reddi et al. (2020) improved the server-side optimization further by using adaptive optimizers with momentum. Khanduri et al. (2021); Karimireddy et al. (2020) proposed to perform momentum updates both centrally on the server and locally on the clients. Sun et al. (2023) introduced multistage FedGM which interpolates between FedAvg and FedAvgM with a hyperparameter scheduler, and provides a general momentum computation for FL to better control the momentum acceleration. Our approach is orthogonal to these works and compatible to any momentum-based optimizers.

## 6. Conclusion

We demonstrate how stale model updates incur an implicit bias in AsyncFL, which diminishes the acceleration from momentum-based optimizers. To address this issue, we propose momentum approximation which optimizes a least square problem online to find the optimal weighted average of historical model updates that approximates the desired momentum updates. Momentum approximation is easy to integrate in production FL systems with a minor storage and communication cost. We empirically evaluate momentum approximation in both non-private and private settings on real-world benchmark FL datasets, and demonstrated that it outperforms the existing AsyncFL algorithms.



## Impact Statements

This work does not have negative societal or ethical impact. On the contrary, this work can potentially benefit the society in terms of stronger privacy protection. Our proposed method is compatible with secure aggregation and differential privacy, and can be easily integrated to existing asynchronous federated learning production systems. We believe that our method can improve the applicability of asynchronous private federated learning to more on-device ML products where the data is highly personal and sensitive, and thus provide meaningful privacy guarantee to the end users.

## References

- Abadi, M., Chu, A., Goodfellow, I., McMahan, H. B., Mironov, I., Talwar, K., and Zhang, L. Deep learning with differential privacy. In *Proceedings of the 2016 ACM SIGSAC conference on computer and communications security*, pp. 308–318, 2016.
- Authors, T. T. F. Tensorflow federated stack overflow dataset. [https://www.tensorflow.org/federated/api\\_docs/python/tff/simulation/datasets/stackoverflow/load\\_data](https://www.tensorflow.org/federated/api_docs/python/tff/simulation/datasets/stackoverflow/load_data), 2019.
- Barkai, S., Hakimi, I., and Schuster, A. Gap aware mitigation of gradient staleness. *arXiv preprint arXiv:1909.10802*, 2019.
- Bonawitz, K., Ivanov, V., Kreuter, B., Marcedone, A., McMahan, H. B., Patel, S., Ramage, D., Segal, A., and Seth, K. Practical secure aggregation for privacy-preserving machine learning. In *proceedings of the 2017 ACM SIGSAC Conference on Computer and Communications Security*, pp. 1175–1191, 2017.
- Bonawitz, K., Eichner, H., Grieskamp, W., Huba, D., Ingerman, A., Ivanov, V., Kiddon, C., Konečný, J., Mazzocchi, S., McMahan, B., et al. Towards federated learning at scale: System design. *Proceedings of machine learning and systems*, 1:374–388, 2019.
- Chai, Z., Chen, Y., Anwar, A., Zhao, L., Cheng, Y., and Rangwala, H. Fedat: A high-performance and communication-efficient federated learning system with asynchronous tiers. In *Proceedings of the International Conference for High Performance Computing, Networking, Storage and Analysis*, pp. 1–16, 2021.
- Chen, Y., Sun, X., and Jin, Y. Communication-efficient federated deep learning with layerwise asynchronous model update and temporally weighted aggregation. *IEEE transactions on neural networks and learning systems*, 31(10): 4229–4238, 2019.
- Chen, Y., Ning, Y., Slawski, M., and Rangwala, H. Asynchronous online federated learning for edge devices with non-iid data. In *2020 IEEE International Conference on Big Data (Big Data)*, pp. 15–24. IEEE, 2020.
- Choquette-Choo, C. A., Ganesh, A., McKenna, R., McMahan, H. B., Rush, K., Thakurta, A. G., and Xu, Z. (amplified) banded matrix factorization: A unified approach to private training. *Advances in Neural Information Processing Systems*, 2023.
- De, S., Berrada, L., Hayes, J., Smith, S. L., and Balle, B. Unlocking high-accuracy differentially private image classification through scale. *arXiv preprint arXiv:2204.13650*, 2022.
- Denisov, S., McMahan, H. B., Rush, J., Smith, A., and Guha Thakurta, A. Improved differential privacy for sgd via optimal private linear operators on adaptive streams. *Advances in Neural Information Processing Systems*, 35: 5910–5924, 2022.
- Duchi, J., Hazan, E., and Singer, Y. Adaptive subgradient methods for online learning and stochastic optimization. *Journal of machine learning research*, 12(7), 2011.
- Dun, C., Hipolito, M., Jermaine, C., Dimitriadis, D., and Kyriilidis, A. Efficient and light-weight federated learning via asynchronous distributed dropout. In *International Conference on Artificial Intelligence and Statistics*, pp. 6630–6660. PMLR, 2023.
- Dutta, S., Wang, J., and Joshi, G. Slow and stale gradients can win the race. *IEEE Journal on Selected Areas in Information Theory*, 2(3):1012–1024, 2021.
- Dwork, C. and Roth, A. The algorithmic foundations of differential privacy. *Foundations and Trends® in Theoretical Computer Science*, 9(3–4):211–407, 2014.
- Dwork, C., Kenthapadi, K., McSherry, F., Mironov, I., and Naor, M. Our data, ourselves: Privacy via distributed noise generation. In *Advances in Cryptology-EUROCRYPT 2006: 24th Annual International Conference on the Theory and Applications of Cryptographic Techniques, St. Petersburg, Russia, May 28-June 1, 2006. Proceedings 25*, pp. 486–503. Springer, 2006a.
- Dwork, C., McSherry, F., Nissim, K., and Smith, A. Calibrating noise to sensitivity in private data analysis. In *Theory of Cryptography: Third Theory of Cryptography Conference, TCC 2006, New York, NY, USA, March 4-7, 2006. Proceedings 3*, pp. 265–284. Springer, 2006b.
- Gupta, V., Koren, T., and Singer, Y. Shampoo: Preconditioned stochastic tensor optimization. In *International Conference on Machine Learning*, pp. 1842–1850. PMLR, 2018.

- Hakimi, I., Barkai, S., Gabel, M., and Schuster, A. Taming momentum in a distributed asynchronous environment. *arXiv preprint arXiv:1907.11612*, 2019.
- He, K., Zhang, X., Ren, S., and Sun, J. Deep residual learning for image recognition. In *Proceedings of the IEEE conference on computer vision and pattern recognition*, pp. 770–778, 2016.
- Hsu, T.-M. H., Qi, H., and Brown, M. Measuring the effects of non-identical data distribution for federated visual classification. *arXiv preprint arXiv:1909.06335*, 2019.
- Huba, D., Nguyen, J., Malik, K., Zhu, R., Rabbat, M., Yousefpour, A., Wu, C.-J., Zhan, H., Ustinov, P., Srinivas, H., et al. Papaya: Practical, private, and scalable federated learning. *Proceedings of Machine Learning and Systems*, 4:814–832, 2022.
- Kairouz, P., McMahan, B., Song, S., Thakkar, O., Thakurta, A., and Xu, Z. Practical and private (deep) learning without sampling or shuffling. In *International Conference on Machine Learning*, pp. 5213–5225. PMLR, 2021.
- Karimireddy, S. P., Jaggi, M., Kale, S., Mohri, M., Reddi, S. J., Stich, S. U., and Suresh, A. T. Mime: Mimicking centralized stochastic algorithms in federated learning. *arXiv preprint arXiv:2008.03606*, 2020.
- Khanduri, P., Sharma, P., Yang, H., Hong, M., Liu, J., Rajawat, K., and Varshney, P. Stem: A stochastic two-sided momentum algorithm achieving near-optimal sample and communication complexities for federated learning. *Advances in Neural Information Processing Systems*, 34:6050–6061, 2021.
- Kingma, D. P. and Ba, J. Adam: A method for stochastic optimization. In *International Conference on Learning Representations*, 2015.
- Kosson, A., Chiley, V., Venigalla, A., Hestness, J., and Koster, U. Pipelined backpropagation at scale: training large models without batches. *Proceedings of Machine Learning and Systems*, 3:479–501, 2021.
- Li, M., Chen, Y., Wang, Y., and Pan, Y. Efficient asynchronous vertical federated learning via gradient prediction and double-end sparse compression. In *2020 16th international conference on control, automation, robotics and vision (ICARCV)*, pp. 291–296. IEEE, 2020.
- Li, T., Zaheer, M., Liu, K., Reddi, S. J., McMahan, H. B., and Smith, V. Differentially private adaptive optimization with delayed preconditioners. In *International Conference on Learning Representations*, 2023.
- Lu, X., Liao, Y., Lio, P., and Hui, P. Privacy-preserving asynchronous federated learning mechanism for edge network computing. *IEEE Access*, 8:48970–48981, 2020.
- McMahan, B., Moore, E., Ramage, D., Hampson, S., and y Arcas, B. A. Communication-efficient learning of deep networks from decentralized data. In *Artificial intelligence and statistics*, pp. 1273–1282. PMLR, 2017.
- McMahan, H. B., Ramage, D., Talwar, K., and Zhang, L. Learning differentially private recurrent language models. In *International Conference on Learning Representations*, 2018.
- Melis, L., Song, C., De Cristofaro, E., and Shmatikov, V. Exploiting unintended feature leakage in collaborative learning. In *2019 IEEE symposium on security and privacy (SP)*, pp. 691–706. IEEE, 2019.
- Mironov, I. Rényi differential privacy. In *2017 IEEE 30th computer security foundations symposium (CSF)*, pp. 263–275. IEEE, 2017.
- Mironov, I., Talwar, K., and Zhang, L. Rényi differential privacy of the sampled gaussian mechanism. *arXiv preprint arXiv:1908.10530*, 2019.
- Mitliagkas, I., Zhang, C., Hadjis, S., and Ré, C. Asynchrony begets momentum, with an application to deep learning. In *2016 54th Annual Allerton Conference on Communication, Control, and Computing (Allerton)*, pp. 997–1004. IEEE, 2016.
- Nasr, M., Shokri, R., and Houmansadr, A. Comprehensive privacy analysis of deep learning: Passive and active white-box inference attacks against centralized and federated learning. In *2019 IEEE symposium on security and privacy (SP)*, pp. 739–753. IEEE, 2019.
- Nguyen, J., Malik, K., Zhan, H., Yousefpour, A., Rabbat, M., Malek, M., and Huba, D. Federated learning with buffered asynchronous aggregation. In *International Conference on Artificial Intelligence and Statistics*, pp. 3581–3607. PMLR, 2022.
- Park, J., Han, D.-J., Choi, M., and Moon, J. Sageflow: Robust federated learning against both stragglers and adversaries. *Advances in neural information processing systems*, 34:840–851, 2021.
- Paulik, M., Seigel, M., Mason, H., Telaar, D., Kluivers, J., van Dalen, R., Lau, C. W., Carlson, L., Granqvist, F., Vandeveld, C., et al. Federated evaluation and tuning for on-device personalization: System design & applications. *arXiv preprint arXiv:2102.08503*, 2021.
- Reddi, S. J., Charles, Z., Zaheer, M., Garrett, Z., Rush, K., Konečný, J., Kumar, S., and McMahan, H. B. Adaptive federated optimization. In *International Conference on Learning Representations*, 2020.

- Song, C., Granqvist, F., and Talwar, K. Flair: Federated learning annotated image repository. *Advances in Neural Information Processing Systems*, 35:37792–37805, 2022.
- Sun, J., Wu, X., Huang, H., and Zhang, A. On the role of server momentum in federated learning. *arXiv preprint arXiv:2312.12670*, 2023.
- Talwar, K., Wang, S., McMillan, A., Jina, V., Feldman, V., Basile, B., Cahill, A., Chan, Y. S., Chatzidakis, M., Chen, J., et al. Samplable anonymous aggregation for private federated data analysis. *arXiv preprint arXiv:2307.15017*, 2023.
- van Dijk, M., Nguyen, N. V., Nguyen, T. N., Nguyen, L. M., Tran-Dinh, Q., and Nguyen, P. H. Asynchronous federated learning with reduced number of rounds and with differential privacy from less aggregated gaussian noise. *arXiv preprint arXiv:2007.09208*, 2020.
- Vaswani, A., Shazeer, N., Parmar, N., Uszkoreit, J., Jones, L., Gomez, A. N., Kaiser, Ł., and Polosukhin, I. Attention is all you need. *Advances in neural information processing systems*, 30, 2017.
- Wang, E., Chen, B., Chowdhury, M., Kannan, A., and Liang, F. Flint: A platform for federated learning integration. *Proceedings of Machine Learning and Systems*, 5, 2023.
- Wang, J., Tantia, V., Ballas, N., and Rabbat, M. Slowmo: Improving communication-efficient distributed sgd with slow momentum. *arXiv preprint arXiv:1910.00643*, 2019a.
- Wang, J., Charles, Z., Xu, Z., Joshi, G., McMahan, H. B., Al-Shedivat, M., Andrew, G., Avestimehr, S., Daly, K., Data, D., et al. A field guide to federated optimization. *arXiv preprint arXiv:2107.06917*, 2021a.
- Wang, Q., Li, Q., Wang, K., Wang, H., and Zeng, P. Efficient federated learning for fault diagnosis in industrial cloud-edge computing. *Computing*, 103(10):2319–2337, 2021b.
- Wang, S., Tuor, T., Salonidis, T., Leung, K. K., Makaya, C., He, T., and Chan, K. Adaptive federated learning in resource constrained edge computing systems. *IEEE journal on selected areas in communications*, 37(6):1205–1221, 2019b.
- Xie, C., Koyejo, S., and Gupta, I. Asynchronous federated optimization. *arXiv preprint arXiv:1903.03934*, 2019.
- Xu, M., Song, C., Tian, Y., Agrawal, N., Granqvist, F., van Dalen, R., Zhang, X., Argueta, A., Han, S., Deng, Y., et al. Training large-vocabulary neural language models by private federated learning for resource-constrained devices. In *ICASSP 2023-2023 IEEE International Conference on Acoustics, Speech and Signal Processing (ICASSP)*, pp. 1–5. IEEE, 2023a.
- Xu, Z., Zhang, Y., Andrew, G., Choquette-Choo, C. A., Kairouz, P., McMahan, H. B., Rosenstock, J., and Zhang, Y. Federated learning of gboard language models with differential privacy. In *Proceedings of the 61st Annual Meeting of the Association for Computational Linguistics (Volume 5: Industry Track)*, 2023b.
- Yang, H., Fang, M., and Liu, J. Achieving linear speedup with partial worker participation in non-iid federated learning. *International Conference on Learning Representations*, 2021.
- Zhang, F., Liu, X., Lin, S., Wu, G., Zhou, X., Jiang, J., and Ji, X. No one idles: Efficient heterogeneous federated learning with parallel edge and server computation. In *International Conference on Machine Learning*, pp. 41399–41413. PMLR, 2023.
- Zhang, J. and Mitliagkas, I. Yellowfin and the art of momentum tuning. *arXiv preprint arXiv:1706.03471*, 2017.
- Zhang, W., Gupta, S., Lian, X., and Liu, J. Staleness-aware async-sgd for distributed deep learning. In *Proceedings of the Twenty-Fifth International Joint Conference on Artificial Intelligence*, pp. 2350–2356, 2016.
- Zheng, S., Meng, Q., Wang, T., Chen, W., Yu, N., Ma, Z.-M., and Liu, T.-Y. Asynchronous stochastic gradient descent with delay compensation. In *International Conference on Machine Learning*, pp. 4120–4129. PMLR, 2017.
- Zhu, L., Liu, Z., and Han, S. Deep leakage from gradients. *Advances in neural information processing systems*, 32, 2019.
- Zhu, Y. and Wang, Y.-X. Poission subsampled rényi differential privacy. In *International Conference on Machine Learning*, pp. 7634–7642. PMLR, 2019.

## A. Additional Details in Momentum Approximation

### A.1. Asynchronous sampling noise

To help understand the impact of asynchronous sampling noise in Equation (7), we define

$$\mathbf{d}_t^* = \frac{1}{m} \sum_{k=1}^m \Delta_k(\boldsymbol{\theta}_t), \quad (20)$$

i.e. the average of local model updates from all  $m$  clients. We also have the following assumptions which are common in AsyncFL literature (Wang et al., 2019b; Yang et al., 2021; Nguyen et al., 2022).

**Assumption A.1** (Bounded Dissimilarity). For all clients  $k \in [m]$  and for each iteration  $t$ ,  $\|\Delta_k(\boldsymbol{\theta}_t) - \mathbf{d}_t^*\|_2^2 \leq G^2$ .

**Assumption A.2** (Bounded Staleness). For all clients  $k \in [m]$  and for each iteration  $t$ , the staleness  $\tau(k) \leq \tau_{\max}$ .

With Assumption A.1, it is straightforward to see that for any subset of clients  $\mathcal{K} \subseteq [m]$ , their averaged model updates has the following error:

$$\begin{aligned} \left\| \frac{1}{|\mathcal{K}|} \sum_{k \in \mathcal{K}} \Delta_k(\boldsymbol{\theta}_t) - \mathbf{d}_t^* \right\|_2^2 &= \frac{1}{|\mathcal{K}|^2} \left\| \sum_{k \in \mathcal{K}} (\Delta_k(\boldsymbol{\theta}_t) - \mathbf{d}_t^*) \right\|_2^2 \\ &\leq \frac{1}{|\mathcal{K}|} \sum_{k \in \mathcal{K}} \|\Delta_k(\boldsymbol{\theta}_t) - \mathbf{d}_t^*\|_2^2 = G^2. \end{aligned} \quad (21)$$

Let  $\mathcal{K}_s$  be a Poisson sampled set of clients at iteration  $s$ ,  $\mathcal{K}_{t,s} \subseteq \mathcal{K}_s$  be a subset of clients whose model update received at iteration  $t \geq s$  and  $C_{t,s} = |\mathcal{K}_{t,s}|$ . Then the sampling noise in Equation (6) can be quantified as:

$$\boldsymbol{\zeta}_{t,s} = \frac{1}{C_{t,s}} \sum_{k \in \mathcal{K}_{t,s}} \Delta_k(\boldsymbol{\theta}_s) - \mathbf{d}_t. \quad (22)$$

Then with Equation (21), the  $L^2$  norm of the sampling noise can be bounded as:

$$\begin{aligned} \|\boldsymbol{\zeta}_{t,s}\|_2^2 &= \left\| \frac{1}{C_{t,s}} \sum_{k \in \mathcal{K}_{t,s}} \Delta_k(\boldsymbol{\theta}_s) - \mathbf{d}_t^* + \mathbf{d}_t^* - \mathbf{d}_t \right\|_2^2 \\ &\leq 2 \left\| \frac{1}{C_{t,s}} \sum_{k \in \mathcal{K}_{t,s}} \Delta_k(\boldsymbol{\theta}_s) - \mathbf{d}_t^* \right\|_2^2 + 2 \|\mathbf{d}_t^* - \mathbf{d}_t\|_2^2 \leq 4G^2. \end{aligned} \quad (23)$$

Given that  $\sum_{s=t-\tau_{\max}}^t \frac{C_{t,s}}{C} = 1$ , we can bound the Frobenius norm of  $\mathbf{E}$  in Equation (7) as:

$$\begin{aligned} \|\mathbf{E}\|_F^2 &= \sum_{t=1}^T \left\| \sum_{s=t-\tau_{\max}}^t \frac{C_{t,s}}{C} \boldsymbol{\zeta}_{t,s} \right\|_2^2 \leq \sum_{t=1}^T (\tau_{\max} + 1) \sum_{s=t-\tau_{\max}}^t \left\| \frac{C_{t,s}}{C} \boldsymbol{\zeta}_{t,s} \right\|_2^2 \\ &\leq \sum_{t=1}^T (\tau_{\max} + 1) \sum_{s=t-\tau_{\max}}^t \frac{C_{t,s}}{C} 4G^2 = \mathcal{O}(\tau_{\max} T G^2), \end{aligned} \quad (24)$$

which suggests that the sampling noise scales linearly with staleness bound  $\tau_{\max}$ . We leave it to future work to investigate proper ways to alleviate the error from asynchronous sampling.

### A.2. Implicit bias in preconditioner

For adaptive optimizers such as Adam (Kingma & Ba, 2015) and RMSProp, the preconditioner  $\mathbf{H}_t$  is the square root of exponentially decaying average of the gradients' second moments:

$$\text{diag}(\mathbf{H}_t)^2 \leftarrow \beta' \text{diag}(\mathbf{H}_t)^2 + (1 - \beta') \mathbf{r}_t^2. \quad (25)$$

The stale updates in  $\mathbf{r}_t$  bias the estimation of second moments similar to the implicit momentum bias term in Equation (7). Nonetheless, preconditioner is known to be robust to delayed gradients (Gupta et al., 2018; Li et al., 2023). We leave the exploration of whether mitigating implicit bias from staleness in the second moments is helpful to future work.

## B. Additional Experiments Details

### B.1. Hyperparameters.

For the FLAIR dataset, we use a ResNet-18 model (He et al., 2016) following the setup in (Song et al., 2022). We train the model for 5,000 iterations with local learning rate set to 0.1, local epochs set to 2, and local batch size set to 16. For the StackOverflow dataset, we use a 3-layer Transformer model (Vaswani et al., 2017) following the setup in (Wang et al., 2021a). We train the model for 2,000 iterations with local learning rate set to 0.3 and local epochs set to 1, and local batch size set to 16. The cohort size  $C$  is set to 200 for both dataset. For FedAvgM, we search the learning rate  $\eta$  between (0.1, 1.0). For FedAdam, we set the  $\beta'$  for the second moment to 0.99 and the adaptivity parameter to 0.01, and search the server learning rate  $\eta$  between (0.01, 0.1).

For DP experiments, we set the  $(\epsilon, \delta)$  privacy budget to  $(2.0, 10^{-7})$ -DP with a simulated population size of  $10^7$  and cohort size of 5,000 following prior work (McMahan et al., 2018). We set the  $L^2$  clipping bound  $S_\Delta$  to 0.1 for FLAIR and 0.2 for StackOverflow. We use amplification by subsampling with Rényi DP to calibrate the Gaussian noise scale  $\sigma$  (Mironov, 2017; Mironov et al., 2019). Though we focus on independent Gaussian mechanism in each iteration, our approach is also compatible with DP-FTRL mechanisms with correlated noise between iterations (Kairouz et al., 2021; Choquette-Choo et al., 2023). For momentum approximation where  $\mathbf{W}$  needs to be estimate privately, we set  $\xi$  in Equation (17) such that  $S = 1.1S_\Delta$ , i.e. we pay 10% extra noise on  $\Delta$  to learn  $\mathbf{W}$  privately with the same budget.

For all experiments, we apply exponential moving average (EMA) on central model parameters  $\theta$  with decay rate of 0.99 (De et al., 2022), and report the metrics evaluated on the EMA model parameters.

### B.2. Weight Prediction Baseline

---

#### Algorithm 2 FedBuff with Weight Prediction

---

**Inputs:** client Poisson sampling rate  $q$ , cohort size  $C$ , server optimizer SERVEROPT, server learning rate  $\eta$ , number of FL iterations  $T$ , client local learning rate  $\eta_l$ , number, number of client local SGD steps  $Q$ ,  $\alpha$  EMA decay parameter for historical model updates  
**while**  $t < T$  **do**

$\mathcal{C}_t \leftarrow$  sampled clients with Poisson sampling rate  $q$   
 Run CLIENT( $\theta_t, t, \eta \mathbf{H}_t^{-1} \mathbf{x}_h$ ) for  $k \in \mathcal{C}_t$  asynchronously  
**if** receives  $\Delta_k(\theta_{t-\tau(k)})$  from  $k$  **then**  
      $\mathbf{x}_t \leftarrow \mathbf{x}_t + \frac{1}{C} \Delta_k(\theta_{t-\tau(k)})$   
**if** received  $C$  results in the buffer **then**  
      $\mathbf{m}_t, \mathbf{H}_t \leftarrow$  update based on SERVEROPT

$\theta_{t+1} \leftarrow \theta_t - \eta \mathbf{H}_t^{-1} \mathbf{m}_t$   
 $\mathbf{x}_h \leftarrow \alpha \mathbf{x}_h + (1 - \alpha) \mathbf{x}_t$   
 $\mathbf{x}_{t+1} \leftarrow \mathbf{0}$   
 $t \leftarrow t + 1$

**function** CLIENT( $\theta, t, \eta \mathbf{H}_t^{-1} \mathbf{x}_h$ )  
 $\tau \leftarrow t' - t$  gets the current staleness  
 $\hat{\theta}_{t+\tau} \leftarrow \theta - \tau \eta \mathbf{H}_t^{-1} \mathbf{x}_h$   
 $\theta' \leftarrow$  run  $Q$  SGD steps with  $\eta_l$  on  $\hat{\theta}_{t+\tau}$   
 Upload  $\Delta = \hat{\theta}_{t+\tau} - \theta'$  to server

---

WP is proposed to speed up asynchronous SGD (Kosson et al., 2021) and in particular, to address the implicit momentum issue (Hakimi et al., 2019). In Algorithm 2, we modify WP to be compatible with adaptive optimizer in FedBuff as another baseline for evaluating momentum approximation. To predict the future model, the server sends both  $\theta_t$  and the historical model updates  $\mathbf{x}_h$  to devices. For a sampled client with staleness  $\tau$ , the client tries to first predict the future model  $\hat{\theta}_{t+\tau} \approx \theta_{t+\tau}$ , by running  $\tau$  steps of SERVEROPT( $\theta, \mathbf{x}_h, \eta$ ). We consider  $\mathbf{x}_h$  to be the exponential decay averaging of  $\mathbf{X}_{:t}$  for variance reduction. For adaptive SERVEROPT such as Adam, we send  $\mathbf{H}_t^{-1} \mathbf{x}_h$  to devices for WP. Client then runs the local SGD steps on  $\hat{\theta}_{t+\tau}$  and returns the model update to the server. Note that this method will also double the communication as the server needs to send extra historical model updates for WP.

### B.3. Additional Results

**Impact of staleness bound  $\tau_{\max}$ .** As showed in Equation (24),  $\tau_{\max}$  increases the sampling error, and we empirically study the impact of  $\tau_{\max}$  on momentum approximation by varying it from 20 to 50. Table 3 summarizes the results on the StackOverflow dataset, where larger  $\tau_{\max}$  leads to lower accuracy. Another observation is that the drop in performance of FedAdam is greater than that of FedAvgM which could be from the impact of staleness on the estimation of preconditioner in FedAdam.

**Impact of client delay distribution.** We evaluate the impact of different client delay distribution on momentum approximation objective in Equation (11). We choose Half-Normal, Uniform and Exponential distribution following Nguyen et al.

$\tau_{\max}$	FedAvgM		FedAam	
	MA	MA-light	MA	MA-light
20	26.36	26.11	26.79	26.45
30	26.26	26.05	26.54	26.24
40	26.15	25.95	26.25	25.87
50	25.97	25.90	26.00	25.46

Table 3. Accuracy (%) with momentum approximation (MA) for different staleness bound  $\tau_{\max}$  on the StackOverflow dataset.

Client delay distribution	MA	MA-light
Half-Normal	2.58%	33.07%
Uniform	8.35%	36.78%
Exponential	2.41%	33.89%

Table 4. Relative least square error in Equation (11) for different client delay distribution.

(2022). We measure the relative least square error as  $\|\mathbf{AW} - \mathbf{M}\|_F^2 / \|\mathbf{M}\|_F^2$  using the setup in Appendix B.1 and report the results in Table 4. The relative error for light-weight approximation is much higher as expected and is more than 30% for all three distributions. The approximation error is worst for Uniform distribution, while it is in the similar range for Half-Normal and Exponential distribution. Uniform client delay distribution is unrealistic in production FL system and thus our method is robust to different sensible client delay distributions.